

Iterative MIMO Multi-User Detection: Performance Evaluation with COST 259 Channel Model

Helmut Hofstetter, Thomas Zemen, Joachim Wehinger
 ftw. Telecommunication Research Center Vienna, Donau City Str. 1,
 A-1220 Vienna, Austria
 e-mail: hofstetter, zemen, wehinger@ftw.at

Gerhard Steinböck
 ARC Seibersdorf research GmbH, Donau City Str. 1,
 A-1220 Vienna, Austria
 e-mail: gerhard.steinboeck@arcs.ac.at

Abstract—This paper evaluates the performance of a multi-user MIMO detector for various channel models. An implementation of the COST 259 channel model is used in comparison to a simple stochastic tapped delay line model. The performance of the receiver using the various channel models is shown for varying number of users and varying antenna spacings. The receiver has no knowledge about the detailed autocorrelation and power delay profile of the channel, only a maximum velocity of the mobile station and a maximum essential support of the impulse response is assumed.

Keywords—MIMO, Multi-User Detection, COST 259, Channel Model

I. INTRODUCTION

We investigate the performance of an iterative multiple-input multiple-output (MIMO) multi-user receiver in the uplink. Each mobile station uses one transmit antenna. Multi-carrier code division multiple access (MC-CDMA) based on orthogonal frequency division multiplexing (OFDM) is applied using a specific random spreading sequence in the frequency domain. The base station employs more than one antenna. The receiver has no knowledge about the detailed autocorrelation and power delay profile of the channel, only a maximum velocity of the mobile station and a maximum essential support of the impulse response is assumed. We compare the performance of the MIMO multi-user receiver for two scenarios:

- The first is a conventional Rayleigh fading channel, modelled as chip spaced delay tap line with i.i.d taps and an exponentially decaying power delay profile. The channel is time-variant. Each tap has an autocorrelation according to Jakes' model [8]. The antennas at the base station are assumed to be uncorrelated [9].
- The second scenario is defined by a geometry based stochastic channel model (GSCM) based on the COST 259 recommendations.

We will present the details of the GSCM in the next section and discuss its implementation. Section III discusses the receive algorithm followed by the description of the simulation environment. In Section V results on the performance of the receive algorithm are given. Conclusions are drawn in Section VI.

II. COST 259 CHANNEL MODEL

COST has a long tradition in specifying channel models for wireless applications. The first models were introduced in COST 207 [1]. These models were used for the standardization of GSM. They use simple tap delay line structures. The successor of this action, COST 231 [2], focused on path loss models. The resulting COST Walfish-Ikegami and COST Hata models are still in use for many applications. Within COST 259 [10] the spatial structure of the radio channel was taken into account. This step is important for investigations on multi antenna systems. Within COST 259 the double directional channel was introduced [4].

The principle of our implementation of the COST 259 model, the GSCM [6], is shown in Fig. 1. One or several mobile stations

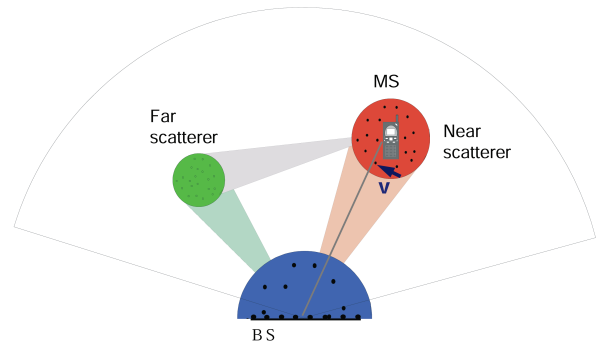


Fig. 1. GSCM principle.

(MS) are placed within the simulation area. The region covers a set of base stations (BS) each having several antennas. A velocity vector is assigned to each MS and near scatterers are placed around the MS. In addition to the scatterers round the MS far scatterers are placed within the simulation area. Such additional scatterers are important for achieving higher delay spreads. The scatterers are grouped into clusters. For each cluster an angular delay power spectra (ADPS) is defined. We use the following definition of a cluster: *A cluster is a set of scatterers having common long term properties, but are not necessarily located closely together.*

This definition matches the definitions of angular- and delay-spread given in COST259. A cluster may encompass an area of several hundred meters in a macro cellular environment. Specular reflection at the scatterers is assumed and a ray tracing tool calculates the impulse responses by summing up all possible paths,

$$h(t, \tau) = \sum_{r=1}^R \alpha_r(t) \delta(t - \tau_r(t)). \quad (1)$$

Each path is characterized by its time variant attenuation $\alpha_r(t)$ and its time variant delay $\tau_r(t)$. R denotes the total number of paths in a scenario. A path starts at the transmitter and is bounced at one or two scatterers before hitting the receiver. The length of the path is used to calculate the delay.

For calculating the magnitude several parameters are taken into account:

$$\alpha_r(t) = L(\Upsilon) \Gamma(t) \Theta(\chi, ADPS). \quad (2)$$

L denotes the path loss given by the path loss model. This parameter mainly depends on the position of the user in the cell. Γ keeps the variations due to the large scale fading and Θ weights the paths according to the scatterer position χ in relation to the positions of the user (Υ) and the BS. Within COST 259 exponential decay in τ and Laplacian shape in azimuth is specified. The transformation of the APDS into the weights is shown in [5]. The computation for far scatterers is the same as for the local ones. In any case, scatterers are not placed according to topographic maps.

For the line-of-sight (LOS) component Θ is replaced by the time variant Rice factor $K(t)$. To ensure that the statistics of the receive power is Rician and not pure Rayleigh at least a quasi-LOS (QLOS) component exists all the time. A more detailed description on the implementation of the model is given in [3]. For OFDM systems, correct modelling of the Doppler variation of the receive signal is very important. The geometric nature of the channel model computes the Doppler implicitly by the movement of the mobiles and the resulting varying lengths of the ray-tracing paths.

For extensive simulations the run-time of the channel model is very important. Calculating the channel impulse response for each chip is not feasible at all. We came up with a structure which calculates the path values α and τ at periodic intersections and use linear interpolation for them in between. The convolution of the channel with the input signal is done on a path by path basis. With this structure an update is only needed after the user has moved about half the wavelength.

In contrast to many other channel models our model does not use a quantized tap-delay line structure, where paths occur exactly within one delay bin only. The delays in our model vary over time due to the movement of the users and the changing lengths of the traced paths. This effect causes problems to simple receive algorithms which assume quantized delays of paths. However assuming quantized delays does not reflect reality and may result in unrealistic good performance of the receive algorithm.

To include this effect sampling at chip rate is not sufficient. In our case we use a four times oversampled input signal for the channel model. This signal is filtered using a root raised cosine filter. Inside the channel model an even higher sample rate is used. At the output of the model the four times over sampled signal is again root raised cosine filtered and down converted to the chip rate for the receiver.

III. ITERATIVE MIMO MULTI-USER RECEIVER FOR TIME-VARIANT CHANNELS

The variation of a wireless channel over the duration of a data block is caused by user mobility and multipath propagation. The Doppler shifts on the individual paths depend on the user's velocity v , the carrier frequency f_C , and the scattering environment. The maximum variation in time of the wireless channel is upper bounded by the maximum (one sided) normalized Doppler bandwidth

$$\nu_{D\max} = B_D T_S, \quad (3)$$

where $B_D = \frac{v_{\max} f_C}{c_0}$ is the maximum Doppler bandwidth, v_{\max} is the maximum velocity, T_S is the symbol duration, and c_0 denotes the speed of light.

We apply orthogonal frequency division multiplexing (OFDM) in order to transform the time-variant frequency-selective channel into a set of parallel time-variant frequency-flat channels, the so-called subcarriers. We consider time-variant channels which may vary significantly over the duration of a long block of OFDM symbols. However, for the duration of each single OFDM symbol, the channel variation is assumed small enough to be neglected. This implies a very small inter-carrier interference (ICI) [11], [9]. Each OFDM symbol is preceded by a cyclic prefix to avoid inter-symbol interference (ISI).

The discrete-time sequence of channel coefficients for each frequency-flat subcarrier is bandlimited by $\nu_{D\max}$. It was shown by Slepian [12] that time-limited parts of bandlimited sequences span a low-dimensional subspace. A natural set of basis functions for this subspace is given by the so-called discrete prolate spheroidal sequences. A Slepian basis expansion using this subspace representation was proposed in [13] for time-variant channel equalization. It was shown in [14] that the channel estimation bias obtained with the Slepian basis expansion is more than a magnitude smaller

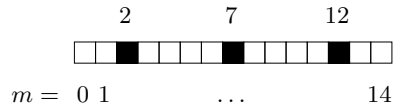


Fig. 2. Example pilot pattern $\mathcal{P} = \{2, 7, 12\}$ defined by (4) for $M = 15$ and $J = 3$.

compared to the Fourier basis expansion (i.e. a truncated discrete Fourier transform) [15].

We apply the iterative time-variant channel estimation scheme developed in [16], [17] to the MIMO case [9] and extend it to multipath channels with non chip-spaced path delays.

A. Signal Model for Doubly Selective Channels.

Every user has a single $N_T = 1$ transmit antenna, the base station has N_R receive antennas. There are K users. We consider the equalization and detection problem for such a $K \times N_R$ multiuser MIMO communications system. Each user's data symbols are spread over N subcarriers by means of a user-specific spreading code. The transmission is block-oriented with block length M ; a data block consists of $M - J$ OFDM data symbols and J OFDM pilot symbols.

The data symbols are chosen from a quadrature phase shift keying (QPSK) symbol constellation. The data symbols are given by $b_k[m] \in \{\pm 1 \pm j\} / \sqrt{2}$ for $m \notin \mathcal{P}$ and $b_k[m] = 0$ for $m \in \mathcal{P}$, where the pilot placement is defined by the index set

$$\mathcal{P} = \{ \lfloor M/J(i + 1/2) \rfloor \mid i = 0, \dots, J - 1 \} \quad (4)$$

and discrete time at rate $1/T_S = 1/(PT_C)$ is denoted by m , see Fig. 2. Each OFDM symbol has a length of P chips. After the spreading operation, pilot symbols $\mathbf{p}_k[m] \in \mathbb{C}^N$ with elements $p_k[m, e]$ are added, giving the $N \times 1$ vectors

$$\mathbf{d}_k[m] = \mathbf{s}_k b_k[m] + \mathbf{p}_k[m]. \quad (5)$$

The elements of the pilot symbols $p_k[m, e]$ for $m \in \mathcal{P}$ and $e \in \{0, \dots, N - 1\}$ are randomly chosen from the QPSK symbol set $\{\pm 1 \pm j\} / \sqrt{2N}$. For $m \notin \mathcal{P}$ we define $\mathbf{p}_k[m] = \mathbf{0}_N$. Subsequently, an N -point inverse discrete Fourier transform (IDFT) is carried-out and a cyclic prefix of length G is inserted. An OFDM symbol including the cyclic prefix has length $P = N + G$ chips.

The temporal channel variation for the duration of each single OFDM symbol is small. Under this assumption, we represent the time-variant MIMO channel by the $N \times 1$ vector $\mathbf{g}_{k,q}[m] = \mathbf{F} [h_{k,q}[mP, 0], \dots, h_{k,q}[mP, L - 1]]^T$. The truncated DFT matrix $\mathbf{F} \in \mathbb{C}^{N \times L}$ has elements $[\mathbf{F}]_{i,\ell} = \frac{1}{\sqrt{N}} e^{-j2\pi i \ell / N}$ for $i \in \{0, \dots, N - 1\}$ and $\ell \in \{0, \dots, L - 1\}$. The received signal at the q th antenna element after cyclic prefix removal and DFT is

$$\mathbf{y}_q[m] = \sum_{k=1}^K \text{diag}(\mathbf{g}_{k,q}[m]) \mathbf{d}_k[m] + \mathbf{v}_q[m] \quad (6)$$

where complex additive white Gaussian noise with zero mean and covariance $\sigma_v^2 \mathbf{I}_N$ is denoted by $\mathbf{v}_q[m] \in \mathbb{C}^N$ with elements $v_q[m, e]$. We define the time-variant effective spreading sequences

$$\tilde{\mathbf{s}}_{k,q}[m] = \text{diag}(\mathbf{g}_{k,q}[m]) \mathbf{s}_k, \quad (7)$$

and the time-variant effective spreading matrix $\tilde{\mathbf{S}}_q[m] = [\tilde{\mathbf{s}}_{1,q}[m], \dots, \tilde{\mathbf{s}}_{K,q}[m]] \in \mathbb{C}^{N \times K}$. Using these definitions, we write the signal model for data detection as

$$\mathbf{y}_q[m] = \tilde{\mathbf{S}}_q[m] \mathbf{b}[m] + \mathbf{v}_q[m] \quad \text{for } m \notin \mathcal{P} \quad (8)$$

where $\mathbf{b}[m] = [b_1[m], \dots, b_K[m]]^T \in \mathbb{C}^K$ contains the stacked data symbols for K users. We apply iterative parallel interference cancellation (PIC) and minimum mean square error (MMSE) filtering as described in [9], [17], [16].

The output of the MMSE filter $w_{k,q}$ of all N_R receive antennas is maximum ratio combined according to

$$z_k[m] = \frac{\sum_{q=1}^{N_R} w_{k,q}[m] \|\mathbf{g}_{k,q}[m]\|^2}{\sum_{q=1}^{N_R} \|\mathbf{g}_{k,q}[m]\|^2}. \quad (9)$$

The soft decision $z_k[m]$ is used as input to the BCJR decoder. For more details on the decoder see [9], [18].

The performance of the iterative receiver crucially depends on the accuracy with which the time-variant frequency response $\mathbf{g}_{k,q}[m]$ is estimated, since the effective spreading sequence (7) directly depends on the actual channel realizations. The MIMO-OFDM signal model (6) describes a transmission over $N \times N_R$ parallel frequency-flat channels. Therefore, we rewrite (6) as a set of equations for every subcarrier $e \in \{0, \dots, N-1\}$ and receive antenna $q \in \{1, \dots, N_R\}$,

$$y_q[m, e] = \sum_{k=1}^K g_{k,q}[m, e] d_{k,q}[m, e] + v_q[m, e], \quad (10)$$

where $d_k[m, e] = s_k[e] b_k[m] + p_k[m, e]$. The temporal variation of each subcarrier coefficient $g_{k,q}[m, e]$ is bandlimited by the normalized maximum Doppler bandwidth $\nu_{D_{\max}}$. We estimate $g_{k,q}[m, e]$ for an interval with length M using the received sequence $y_q[m, e]$. Slepian [12] analyzed discrete prolate spheroidal (DPS) sequences that are maximally concentrated in a given time interval and to a given bandwidth. Thus, the properties of these DPS sequences are directly relevant to the channel estimation problem. The DPS sequences are *doubly* orthogonal over the index sets $\{-\infty, \dots, \infty\} = \mathbb{Z}$ and $\{0, \dots, M-1\}$. We use the DPS sequences on the index set $\{0, \dots, M-1\}$ to define an orthogonal basis. The index-limited DPS sequences will be termed *Slepian sequences*.

B. Slepian Basis Expansion.

The Slepian basis expansion approximates the sequence $g_{k,q}[m, e]$ by a linear combination of Slepian sequences $u_i[m]$

$$g_{k,q}[m, e] \approx \tilde{g}_{k,q}[m, e] = \sum_{i=0}^{D-1} u_i[m] \psi_{k,q}[i, e], \quad (11)$$

where $m \in \{0, \dots, M-1\}$, $e \in \{0, \dots, N-1\}$ and $\psi_{k,q}[i, e]$ denotes the basis expansion coefficients for subcarrier e . The Slepian sequences $\mathbf{u}_i \in \mathbb{R}^M$ with elements $u_i[m]$ are defined as the eigenvectors of the matrix $\mathbf{C} \in \mathbb{R}^{M \times M}$ defined as $[\mathbf{C}]_{i,\ell} = \frac{\sin[2\pi(i-\ell)\nu_{D_{\max}}]}{\pi(i-\ell)}$ where $i, \ell = 0, 1, \dots, M-1$, i.e.

$$\mathbf{C} \mathbf{u}_i = \lambda_i \mathbf{u}_i. \quad (12)$$

The approximate dimension of the time-concentrated and bandlimited signal space is $D = \lceil 2\nu_{D_{\max}} M \rceil + 1$ [12, Sec. 3.3], which means that the eigenvalues λ_i rapidly decay to zero for $i > D$. In effect, (11) is a reduced-rank representation for time-limited parts (or snapshots) of bandlimited sequences based on deterministic assumptions about $g_{k,q}[m, e]$. For detailed analysis of the estimation error please refer to [16], [19], [20]. Equation (12) is not suited for the numerical calculation of \mathbf{u}_i because matrix \mathbf{C} is rank deficient. However, there exist other ways to calculate \mathbf{u}_i numerically, see [12] and [21, Section 8.3].

We emphasize that the selection of a suitable Slepian basis, parameterized by M and $\nu_{D_{\max}}$, exploits the band-limitation of the Doppler spectrum to $\nu_{D_{\max}}$ only. The details of the Doppler spectrum for $|\nu| < \nu_{D_{\max}}$ are irrelevant. Our approach therefore differs from a Karhunen-Loève transform which requires *complete* knowledge of the second-order statistics of the fading process. This approach was chosen since MIMO channel sounder measurements have shown that wireless fading channels show stationary behavior for less than 70 wavelengths in a pedestrian urban environment

[22]. We doubt that meaningful short-term fading characteristics (second-order statistics, to begin with) can hardly be acquired in a multiuser MIMO system when users move at vehicular speeds.

C. Time-Variant Channel Estimation with Discrete Prolate Spheroidal Sequences in Two Dimensions

We insert the basis expansion (11) for the coefficients $g_{k,q}[m, e]$ in (10),

$$y_q[m, e] = \sum_{k=1}^K \sum_{i=0}^{D-1} u_i[m] \psi_{k,q}[i, e] d_k[m, e] + v_q[m, e]. \quad (13)$$

We obtain an LMMSE estimate of the subcarrier coefficients $\hat{\psi}_{k,q}[i, e]$ for all K users but individually for every subcarrier e and receive antenna q as described in [9], [16].

After $\hat{\psi}_{k,q}$ is evaluated for all $e \in \{0, \dots, N-1\}$ and $q \in \{1, \dots, N_R\}$, an estimate for the time-variant frequency response is given by $\hat{g}'_{k,q}[m, e] = \sum_{i=0}^{D-1} u_i[m] \hat{\psi}_{k,q}[i, e]$. Additional noise suppression is obtained if we exploit the correlation between the subcarriers.

In the case of a chip-spaced delay tap-line model a simple partial discrete Fourier transform is sufficient [9]. However, the path delays in the geometric channel model (1) are real-valued. Thus, we can write (1) in the frequency domain as

$$g[m, e] = \sum_{r=1}^R \alpha_r(m T_C) e^{-j2\pi\tau_r(m T_C)e/N} \quad (14)$$

for $e \in \{-\infty, \dots, \infty\} = \mathbb{Z}$. We omitted the dependence on k and q . In an OFDM system the channel is estimated in the frequency domain for the subcarriers coefficients $g[m, e]$ for $e \in \{0, \dots, N-1\}$. Thus, the windowing in the frequency domain introduces leakage in the time domain. This situation is dual to the situation described in Section III-B for the estimation problem of a single time-variant flat-fading subcarrier.

In order to accommodate for the leakage, a subspace estimator based on a singular value decomposition of the covariance matrix of $\tilde{\mathbf{g}}_{k,q}$ was presented in [23]. The selection of the subspace dimension was motivated by the concepts introduced by Slepian and proven rigorously in [24]. In [25] the singular value decomposition was calculated in an adaptive manner.

We show in this paper that frequency shifted DPS sequences span the subspace for optimal noise suppression. This is true as long as only an upper bound for the length of the impulse response is assumed. The time delays $\tau_r/(NT_C)$ are from the interval $[0, L_{\max}]$ where $L_{\max} = \max(\tau_r/(NT_C))$. The snapshot length is N . Thus, the corresponding subspace has dimension $D' \geq \lceil L_{\max} \rceil + 1$.

The DPS sequences $\tilde{\mathbf{u}}'_i \in \mathbb{C}^N$ with elements $\tilde{u}'_i[e]$ fulfill (12) when matrix \mathbf{C} is replaced by $[\mathbf{C}']_{i,\ell} = \frac{\sin[2\pi(i-\ell)L_{\max}/2]}{\pi(i-\ell)}$ where $i, \ell = 0, 1, \dots, N-1$. The subspace for noise reduction is spanned by the shifted DPS sequences

$$\mathbf{u}'_i[e] = \tilde{\mathbf{u}}'_i[e] e^{-j2\pi L_{\max} e/(2N)} \quad (15)$$

It can be easily verified that \mathbf{u}'_i are the eigenvectors of the covariance matrix of a uniform power delay profile which is given in [23, Appendix A].

We define

$$\mathbf{f}[e] = \begin{bmatrix} u'_0[(e + N/2) \bmod N] \\ \vdots \\ u'_{D'-1}[(e + N/2) \bmod N] \end{bmatrix} \in \mathbb{C}^{D'}. \quad (16)$$

for $e \in \{0, \dots, N-1\}$ and N even, for expressing noise suppression in the frequency domain as subspace projection according to

$$\hat{g}_{k,q}[m, e] = \mathbf{f}^T[e] \sum_{e'=0}^{N-1} \mathbf{f}^*[e'] \hat{g}'_{k,q}[m, e']. \quad (16)$$

Parameter	Value
Cell size	1000m
No. of base stations	1
No. of BS antennas	{1, 2}
No. of mobile stations	{1, 32}
No. of MS antennas	1
Antenna pattern	omni-directional
Mobile speed	70 km/h
No. of scatterers	20 per cluster
Chip rate	$3.84 \cdot 10^6$ 1/s
Oversampling	4times

Tab. 1. Simulation parameters.

Finally, the data is detected by inserting the channel estimates $\hat{g}_{k,q}[m]$ into (7).

IV. SIMULATION ENVIRONMENT

A. Description of Statistical Simulation Environment

Realizations of the time-variant frequency-selective MIMO channel $h_{k,q}[n, \ell]$ are generated using an exponentially decaying power-delay profile (PDP) $\eta^2[\ell] = e^{-\ell} / \sum_{\ell'=0}^{L-1} e^{-\ell'}$, $\ell = 0, \dots, L-1$, [10] with essential support of $L = 15$. The time indices n and ℓ correspond to sampling at rate $1/T_C$. The PDP corresponds to a root mean square delay spread $T_D = T_C = 260$ ns for a chip rate of $1/T_C = 3.84 \cdot 10^6$ 1/s. The autocorrelation for every channel tap is given by $R_{hh}[n, \ell] = \eta^2[\ell] J_0(2\pi\nu_D Pn)$ which results in the classical Jakes' spectrum [8]. We simulate the time-variant channel using the model in [26] corrected for low velocities in [27].

B. Simulations Using the GSCM

We have chosen the generalized typical urban (GTU) environment for all simulations using the GSCM. This is one of the four specified macro cellular environments of COST 259. The simulation parameters are given in Table 1. At the transmitter a root raised cosine filter is used for pulse-shaping and at the receiver the same filter is taken. Both filters are applied to the four times over sampled transmit signal. After the receive filter the sample rate is reduced to the chip rate. The receiver performs processing at chip rate. All mobiles are uniformly spread within the cell area. Note that there is a minimum distance between base station and mobile station of 100m due to the definition of the scenario.

1) *Power Control and Fading Effects*: The COST 259 channel model includes large-scale and short-scale effects. The first ones are modelled stochastically, the short scale fading is implicitly given by the superposition of the arriving paths. For the focus of this paper the large scale effects are not taken into account since we assume perfect power control for slow changes of the channel. Thus only short scale effects are visible to the receiver. Figure 3 shows the received power levels for 16 users for one time slot and a mobile speed of 70km/h. The power is normalized to a total receive power of 1 (0dB) on average per user. For the MIMO case the summed up power at the receive antennas is unity on average. With these settings the shadow fading is kept out of the simulation. Focusing on the variation of the receive power of the different users the differences look quiet big. But this is mainly due to the short observation period. All mobiles move over a distance of slightly more than one wavelength within one OFDM frame and the output signal of the GSCM model is divided by the path loss value given from the COST Walfish-Ikegami model. This step is necessary since the Rice factor depends on the actual path loss compared to the free space path loss.

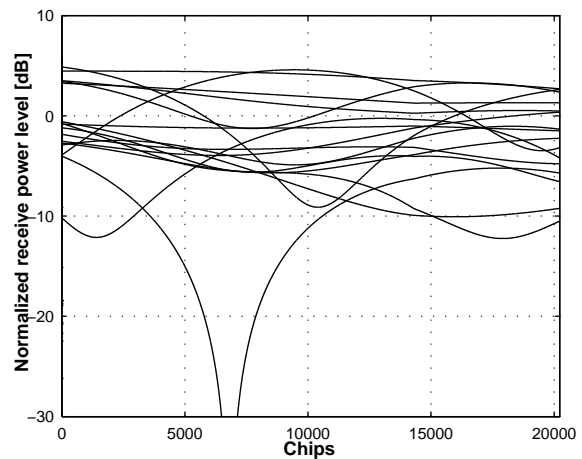


Fig. 3. Normalized receive power of 16 users.

2) *Synchronization*: We assume that all impinging user signals are received at the same time. This is achieved by subtracting the smallest delay from all paths of a user. This is no loss of generality but makes simulations much easier because the receive algorithm does not need additional synchronization measures.

3) *Late Arrivals*: For the GSCM the length of the impulse response is just given by the geometry of the simulated environment. Late arriving components, especially from far clusters, may occur. In an OFDM system the cyclic prefix length determines the maximum path delay that does not lead to performance degradation. To visualize this effect some simulations were performed with and without late arrivals. For the second case all late arriving components were set to zero. The total receive power was kept the same for both cases.

C. System Parameters

The system operates at carrier frequency $f_C = 2$ GHz and the $K = 32$ users move with velocity $v = 70$ km/h. This gives a Doppler bandwidth of $B_D = 133$ Hz corresponding to $\nu_D = 0.0027$. The number of subcarriers is $N = 64$ and the length of the OFDM symbol with cyclic prefix is $P = G + N = 79$. The data block consists of $M = 256$ OFDM symbols with $J = 60$ OFDM pilot symbols. The system is designed for a maximum velocity $v_{max} = 100$ km/h which results in $D = 3$ for the Slepian basis expansion. The base station uses $N_R = \{1, 2\}$ receive antennas. All simulation results are averaged over 100 independently generated data blocks. We assume a maximum path delay of $L_{max} = 10$ and use $D' = 14$ shifted DPS sequences for noise suppression in the frequency domain.

V. RESULTS

In Fig. 4, we illustrate the multiuser MIMO-OFDM uplink performance with iterative time-variant channel estimation based on the Slepian basis expansion in terms of bit error rate (BER) versus E_b/N_0 after 4 iterations. The effect of the statistical and the geometric channel model are compared.

The diversity for both models is nearly the same, which is visible through the slope of the BER versus E_b/N_0 curves. Comparing the statistical model with the GSCM, the too optimistic assumptions of uncorrelated taps and antennas in the statistical model result in better performance. All curves for the statistical model are shifted by about 3dB to the left compared to the GSCM with a receive antenna spacing of 20λ . For 32 users a performance loss of slightly less than 1dB occurs compared to the single user case.

In addition the effect of late arrivals was studied. If the length of the impulse response exceeds the length of the cyclic prefix some

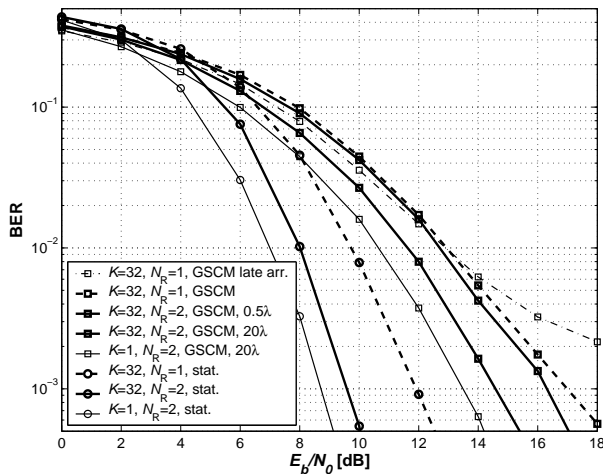


Fig. 4. BER versus SNR on the uplink for multiuser MIMO-OFDM after 4 iterations and Slepian basis expansion for $D = 3$, $K = 32$ users are moving at $v = 70$ km/h, the receiver employs $N_R = 1$ or 2 antennas.

energy is not covered by the receiver. This effect becomes visible for very high E_b/N_0 values. In contrast to the other simulations, which all have the same diversity at high E_b/N_0 , the late arrivals result flatten out.

VI. CONCLUSIONS

Simulation results show that an iterative receiver using the Slepian basis expansion in two dimensions for channel equalization is able to deal with delay tap line models and more realistic GSCM. Our results demonstrate that due to correlations between discrete paths and multiple antennas, which are predicted by the more realistic GSCM, the BER vs E_b/N_0 performance is smaller than for tapped delay line models with independent Rayleigh fading. We show furthermore that detailed statistics are not required for the receiver. Knowledge on the maximum Doppler bandwidth and maximum path delay, however, proves to be valuable.

ACKNOWLEDGEMENTS

This work was carried out with funding from *Kplus* in the ftw projects I0 'Signal and Information Information Processing' and C3 'Smart Antennas for UMTS Frequency Division Duplex' together with Infineon Technologies and ARC Seibersdorf research GmbH.

REFERENCES

- [1] M. Failli (ed.): 'Digital Land Mobile Communications. COST 207 Final Report, 1989, ISBN 92-825-9946-9.
- [2] E. Damosso and L. M. Correia, "Digital mobile radio - towards future generation systems", *final report of COST Action 231, European Union, 1999*.
- [3] H. Hofstetter, G. Steinböck, "A Geometry based Stochastic Channel Model for MIMO Systems", *ITG Workshop on Smart Antennas, Munich, Germany, Jan. 2004*
- [4] Steinbauer et al, "The Double Directional Radio Channel", *IEEE Antennas and Propagation Magazine, August 2001*.
- [5] A.F. Molisch, J. Laurila, and A. Kuchar, "Geometry-base stochastic model for mobile radio channels with directional component", *Proc. 2nd Intelligent Antenna Symp., Univ. Surrey, 9th -10th July 1998*.
- [6] J. Fuhl, A. F. Molisch, and E. Bonek, "Unified channel model for mobile radio systems with smart antennas", *Proc. Inst. Elect. Eng., Radar, Sonar, Navigat., vol. 145, no. 1, pp. 32-41, 1998*.
- [7] H. Hofstetter, A.F. Molisch, M. Steinbauer, "Implementation of a COST259 geometry based stochastic channel model for macro- and microcells", *EPMCC 2001, Vienna, Austria*.
- [8] W. Jakes, *Microwave Mobile Communications*. New York, USA: John Wiley & Sons, 1974.
- [9] C. F. Mecklenbräuker, J. Wehinger, T. Zemen, H. Artés, and F. Hlawatsch, *Smart Antennas in Europe - State of the Art*. EURASIP, Hindawi Publishing Corporation, to appear 2004, ch.1.4 Multiuser MIMO Channel Equalization.

- [10] L. M. Correia, *Wireless Flexible Personalised Communications*. Wiley, 2001.
- [11] Y. G. Li and L. J. Cimini, "Bounds on the interchannel interference of OFDM in time-varying impairments," *IEEE Trans. Commun.*, vol. 49, no. 3, pp. 401–404, March 2001.
- [12] D. Slepian, "Prolate spheroidal wave functions, Fourier analysis, and uncertainty - V: The discrete case," *The Bell System Technical Journal*, vol. 57, no. 5, pp. 1371–1430, May-June 1978.
- [13] T. Zemen and C. F. Mecklenbräuker, "Time-variant channel equalization via discrete prolate spheroidal sequences," in *37th Asilomar Conference on Signals, Systems and Computers*, Pacific Grove (CA), USA, November 2003, pp. 1288–1292, invited.
- [14] —, "Time-variant channel estimation for MC-CDMA using prolate spheroidal sequences," *IEEE Trans. Signal Processing*, revised.
- [15] A. M. Sayeed, A. Sendonaris, and B. Aazhang, "Multiuser detection in fast-fading multipath environment," *IEEE J. Select. Areas Commun.*, vol. 16, no. 9, pp. 1691–1701, December 1998.
- [16] T. Zemen, "OFDM multi-user communication over time-variant channels," Ph.D. dissertation, Vienna University of Technology, Vienna, Austria, August 2004.
- [17] T. Zemen, C. F. Mecklenbräuker, J. Wehinger, and R. R. Müller, "Iterative multi-user decoding with time-variant channel estimation for MC-CDMA," in *Fifth International Conference on 3G Mobile Communication Technologies*, London, United Kingdom, invited, to be presented.
- [18] L. R. Bahl, J. Cocke, F. Jelinek, and J. Raviv, "Optimal decoding of linear codes for minimizing symbol error rate," *IEEE Trans. Inform. Theory*, vol. 20, no. 2, pp. 284–287, Mar. 1974.
- [19] M. Niedzwiecki, *Identification of Time-Varying Processes*. John Wiley & Sons, 2000.
- [20] L. L. Scharf and D. W. Tufts, "Rank reduction for modeling stationary signals," *IEEE Trans. Acoust., Speech, Signal Processing*, vol. ASSP-35, no. 3, pp. 350–355, March 1987.
- [21] D. B. Percival and A. T. Walden, *Spectral Analysis for Physical Applications*. Cambridge University Press, 1963.
- [22] I. Viering and H. Hofstetter, "Potential of coefficient reduction in delay, space and time based on measurements," in *Conference on Information Sciences and Systems (CISS)*, Baltimore, USA, March 2003.
- [23] O. Edfors, M. Sandell, J.-J. van de Beek, S. K. Wilson, and P. O. Börjesson, "OFDM channel estimation by singular value decomposition," *IEEE Trans. Commun.*, vol. 46, no. 7, pp. 931–939, July 1998.
- [24] H. J. Landau and H. O. Pollak, "Prolate spheroidal wave functions, Fourier analysis, and uncertainty -III: The dimension of the space of essentially time- and band-limited signals," *The Bell System Technical Journal*, vol. 41, pp. 1295–1336, June 1962.
- [25] J. Du and Y. G. Li, "D-BLAST OFDM with channel estimation," *EURASIP Journal on Applied Signal Processing*, vol. 5, pp. 605–612, 2004.
- [26] Y. R. Zheng and C. Xiao, "Simulation models with correct statistical properties for Rayleigh fading channels," *IEEE Trans. Commun.*, vol. 51, no. 6, pp. 920–928, June 2003.
- [27] T. Zemen and C. F. Mecklenbräuker, "Doppler diversity in MC-CDMA using the Slepian basis expansion model," in *12th European Signal Processing Conference (EUSIPCO)*, Vienna, Austria, September 2004, to be presented.